RICE UNIVERSITY

A Disposable Bio-nano-chip using Agarose Beads for Protein Analysis

by

Nan Du

A THESIS SUBMITTED
IN PARTIAL FULFILLMENT OF THE
REQUIREMENTS FOR THE DEGREE

Master of Science

APPROVED, THESIS COMMITTEE

John T. McDevitt, Chair
Brown-Wiess Professor of Bioengineering
and Chemistry

Amina A. Qutub
Assistant Professor of Bioengineering

Sibani Lisa Biswal
Assistant Professor of Chemical and
Bimolecular Engineering

HOUSTON, TEXAS
April 2011

Abstract

A Disposable Bio-nano-chip using Agarose Beads for Protein Analysis

by

Nan Du

This thesis reports on the fabrication of a disposable bio-nano-chip (BNC), a microfluidic device composed of polydimethylsiloxane (PDMS) and thiolene-based optical epoxy which is both cost-effective and suitable for high performance immunoassays. A novel room temperature (RT) bonding technique was utilized so as to achieve irreversible covalent bonding between PDMS and thiolene-based epoxy layers, while at the same time being compatible with the insertion of agarose bead sensors, selectively arranged in an array of pyramidal microcavities replicated in the thiolene thin film layer. In the sealed device, the bead-supporting epoxy film is sandwiched between two PDMS layers comprising of fluidic injection and drain channels. The agarose bead sensors used in the device are sensitized with anti-C-reactive protein (CRP) antibody, and a fluorescent sandwich-type immunoassay was run to characterize the performance of this device. Computational fluid dynamics (CFD) was used based on the device specifications to model the bead penetration. Experimental data revealed analyte penetration of the immunocomplex to 100μm into the 280μm diameter agarose beads, which correlated well with the simulation.

A dose response curve was obtained and the linear dynamic range of the assay was established over 1ng/mL to 50ng/mL with a limit of detection less than 1ng/mL.

Acknowledgments

Funding for this work was provided by National Institutes of Health through the National Institute of Dental and Craniofacial Research (U01 DE15017 and U01 DE017793). The content is solely the responsibility of the authors and does not necessarily represent or reflect views of the NIH or the United States Government.

Content

List of Figure

1. Introduction

General immunoassays typically require time-consuming procedures, expensive instruments, and highly trained technicians. In implementing microfabrication techniques, microfluidic technology has shown significant potential to decrease analysis time and miniaturize the large, sophisticated detection instrumentation (Sia and Kricka 2008; Walt 2005). Microfluidic immunoassay systems can target small volumes of biological solutions with highly sensitive integrated sensors (Bange et al. 2005). In efforts to develop portable prototype sensors used in microfluidic systems, researchers have explored various types of functional materials and techniques, such as nitrocellulose paper (Fu et al. 2010), silver reduction (Sia et al. 2004), encoded particles (Pregibon et al. 2007) and gel electrophoresis (Meagher et al. 2008). New signaling strategies, such as multi-wavelength microflow cytometer (Golden et al. 2009), and lensless imaging (Moon et al. 2009) have also been reported to further miniaturize the entire microfluidic systems for point-of-care applications.

Recently, incorporating functionalized colloidal microbeads into microfluidic channels has been reported as a novel miniaturized means to perform immunoassay tests (Lim and Zhang 2007; Shin et al. 2007). As the physical support for capture antibodies (Nolan and Sklar 2002), beads are suitable as sensors for immunoassays. First of all, they possess high surface to volume ratios and thus are capable to immobilize a large number of capture antibodies. Furthermore, because of the fact

that beads are addressable and can be pre-programmed by selective conjugation to various probe molecules, bead-based systems are capable of multiplexed assay tests. While many groups use solid phase beads, such as polystyrene beads, some groups utilize agarose beads (Ali et al. 2003; Christodoulides et al. 2002; Goodey et al. 2001; Jokerst et al. 2008; Thompson et al. 2010), because the interior porous structure of agarose beads, further contributes to increase the number of capture antibodies, and hence antigen antibody interactions (Jokerst et al. 2011).

However, the optimal strategy to integrate agarose beads in microfluidic systems is still not well established yet. As a particular type of gel, agarose beads cannot keep their original shapes if immobilized by clamping in two dimension structures (Thompson and Bau 2010). Further, agarose beads need to be kept moist after preparation to prevent interior pore size degradation upon bead drying (Wong 2007), and it is not quite clear yet whether this will affect final signal stabilities. Moreover, instead of using lateral flow over the top of beads or diffusion driven delivery methods, more complex fluidic patterns such as convective flow are necessary for analytes to quickly and effectively penetrate into the core of the beads to take full advantage of the high avidity and large density of capture antibodies in three dimensional porous structures (Jokerst et al. 2011). To overcome these issues, several studies have employed anisotropically etched silicon to both physically protect beads within dedicated areas of the array and generate convective flow to efficiently deliver analytes to the beads (Christodoulides et al. 2007; Christodoulides et al. 2005b; Jokerst et al. 2010; Jokerst et al. 2009; Kirby et al. 2004; Li et al. 2005;

Sohn et al. 2005). Nevertheless, fabrication issues and cost constraints limit the direct use of silicon into practical systems, and new materials and designs are needed to optimize agarose bead-based immunoassays in microfluidic systems.

This paper focuses on the development of a microfluidic design, termed bio-nano-chip (BNC), composed of PDMS and thiolene-based epoxy, and evaluates its performance with a bead-based C-reactive protein (CRP) immunoassay. The low cost chip was integrated by permanently and irreversibly bonding PDMS and thiolene film at room temperature (RT). The seal-proof chip is disposable and potentially free of contamination. These features are expected to accelerate the translation of the BNC from the laboratories to point of care applications for global public health (Lee et al. 2010; Yager et al. 2006). To characterize the performance of new structure, we carried out a sandwich-type immunoassay for CRP, an inflammation and cardiac risk biomarker (Christodoulides et al. 2005a).

2. Materials and methods

2.1 Materials and Reagents

Silicon wafers (4in.) were purchased from Nova Electronic Materials (Richardson, TX, USA). Photolithography masks were printed on mylar films at 10,160dpi by Fine Line Imaging (Colorado Springs, Colorado, USA). SU8-3035 photoresist was obtained from MicroChem (Newton, MA, USA). Sylgard 184 PDMS

kits were manufactured by Dow Corning (Midland, MI, USA) and 10:1 weight ratio (pre-polymer to curing agent) was used in this work. Norland optical adhesive 81 (NOA81) was ordered from Norland Products (Cranbury, NJ, USA). 3-Aminopropyltriethoxysilane (APTES, 97%) and 2-hydroxyethylmethacrylate (HEMA) were received from Sigma-Aldrich.

Agarose beads were prepared by emulsification of 2% type I-B agarose purchased from Sigma. Briefly, 1g of agarose was stirred and dissolved in 50mL of nano-pure water at 60°C. A suspending solution of 10mL of Span85 (Sigma) and 90mL hexanes was heated to 60°C and stirred at 900rpm. The agarose solution was poured into the suspending solution followed by stirring at 900rpm at 59°C for one minute. The stirring was then adjusted to 600rpm with heat off to allow the agarose to gel to 25°C. Beads were collected, washed with 50/50 mixture of ethanol/water and sorted using a sieve that screens out beads of 250-280μm in diameter, which were then glyoxylated to transform the hydroxyl groups to aldehyde groups.

Rabbit anti-human CRP antibody used both as capture and detection antibody, was purchased from Accurate Chemical Corp (Westbury, NY, USA). AlexaFluor®488 protein labeling kit from Invitrogen was conjugated to the detection antibody following instructions from the manufacturer. CRP antigen was from Fitzgerald (Acton, MA, USA), and the *Helicobacter pylori* antibody conjugated on the control beads, was purchased from Meridian Life Science (Memphis, TN, USA). Prior to the assay, CRP antigen was diluted with phosphate buffered saline (PBS) blocking buffer containing 1% bovine serum albumin (BSA). Secondary

detection antibody was diluted with PBS in 0.4% v/v. A 500 mL volume of glyoxylated 2% agarose beads were coupled to 9mg/mL polyclonal rabbit anti human CRP antibody in a 1.5 mL solution overnight and blocked with tris solution for 1hour prior to final wash. Negative control beads were prepared similarly, by incubating 2% agarose beads with a polyclonal antibody irrelevant to the CRP target and specific to *Helicobacter pylori*.

2.2 Instrumentation

The BNC was placed under a BX2 Olympus microscope, equipped with a mercury lamp, a 0.13 NA 4 x UPlanFlair objective, and a FITC filter cube (fluoroisothiocyanate, 480 nm excitation, 505 nm long-pass beam splitter dichroic mirror, and 535±25 nm emissions). Fluorescent images were captured by a DVC 1312C CCD camera (Digital Video Camera, Austin, TX, USA).

Confocal images were acquired on an LSM 510 META laser scanning microscope system equipped with a 10x/0.45 Plen-APOCHROMAT objective lens from Zeiss (Germany). From the excitation and emission maxima of the AlexaFluor®488 dye at 495 nm and 519 nm, respectively, the proper configuration controls were applied. Argon laser, Lasos Carl Zeiss promenade 10, with output of 50% was used for excitation at 488nm. Fluorescence emission was detected in the interval between 500 nm and 550 nm.

2.3 Assay procedure

In this study, the chip was then structurally and functionally evaluated with the completion of a series of assays targeting detection of CRP. Prior to the assay, a 3×4 microarray of wells on the chip was manually loaded with agarose beads. The first three columns on the array were loaded with beads coupled to anti-CRP antibody, while the fourth column hosted negative control beads, coupled to an irrelevant antibody to CRP antigen. A syringe pump (NE-1000, New Era Pump Systems) was employed to deliver the samples and reagents for the assay. After exciting the beads at 480nm, the CRP detection beads exhibited green fluorescence signals in contrast to the negative counterparts, confirming the specificity of the antigen-antibody reactions and negligible non-specific binding within the BNC device (Figure 2).

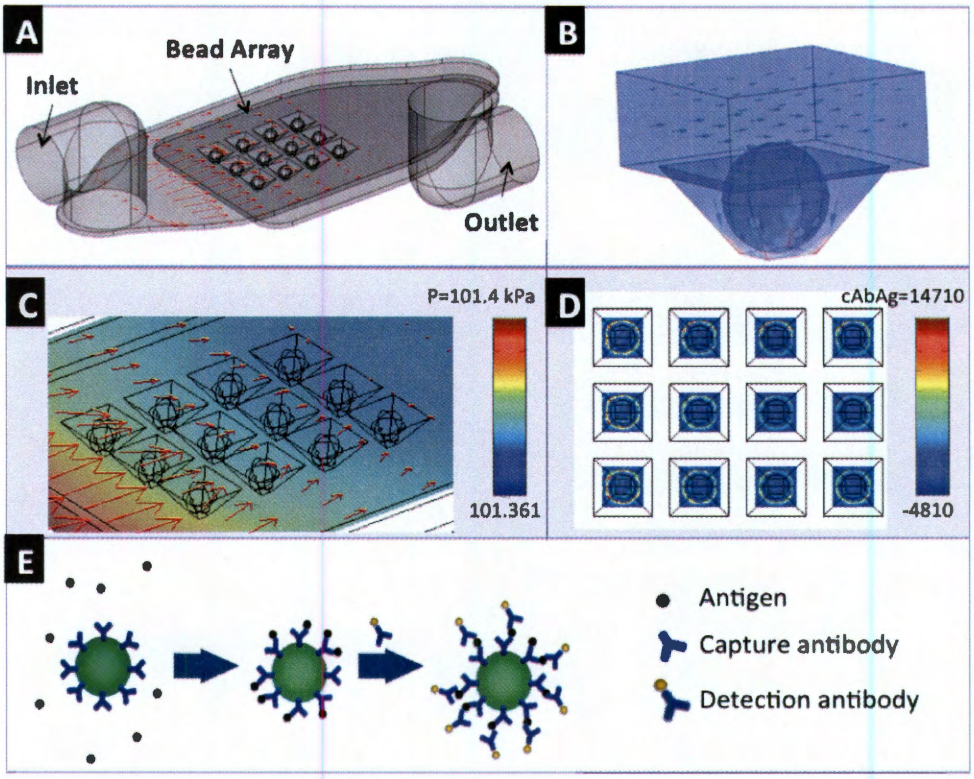

Figure 1 (A) Thiolene-based epoxy bead array layer is sandwiched between two PDMS microfluidic layers. (B) Each 280μm bead rests in a pyramidal pit well replicated from anisotropically etched silicon. (C) A higher pressure exists at the initial bead column closest to the inlet. (D) Computational fluidic dynamics simulations show analyte binding onto the bead array. (E) Schematic representation of a sandwiched-type immunoassay on agarose beads. Individual agarose beads conjugated on their surface and in their interior with a capture antibody are exposed to samples containing the target antigen. The unbound antigen is then washed away and a fluorescence-labeled detection antibody specific to the antigen is added that provides the

characteristic signals when bound to the antigen throughout the beads imaged with a CCD camera.

2.4 Data analysis

The beads were optically excited at 480 nm and resulting images were captured by CCD and further processed to quantitate the signals derived from the beads. More specifically, custom-built image analysis routines written within the ImageJ environment were used to process the captured images and analyze the fluorescence data. Each bead in the array as visualized in the green color was scanned with a series of line profiles spanning 80% of the bead diameter and the average of the maximum obtained for each profile line was recorded into a list. An outlier routine rejected measurements outside two standard deviations (SD) from the median. The fluorescence signal of a bead was calculated by averaging the fluorescence intensity from the remaining measurements. The fluorescence intensity of an array was defined as the average of all fluorescent beads of the same type (i.e., CRP) and the background was defined as the average of the negative control beads.

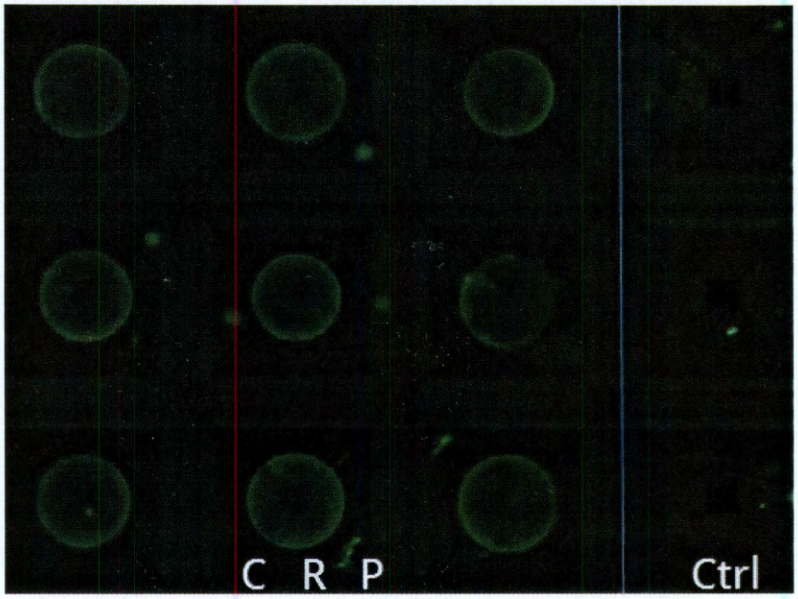

Figure 2 Epi-fluorescence image of bead array at the end of assays (10ng/mL).

2.5 Computational Modeling

Computational simulations were run in COMSOL 3.5a (Burlington, MA). An array of 280 μm beads resting in individual wells was constructed using AutoCAD and then imported into COMSOL. Navier-Stokes and Convection and Diffusion application modes were added from the Chemical Engineering module. The subdomain properties of the beads were loaded from the water library and Brinkman's equation was enabled to allow for flow through a 243nm pore size bead with 96% porosity. The inlet velocity was set to 80 μL/min and outlet pressure was set to atmospheric pressure. The reaction rate governing the system is given by *cAb* + *cAg* <=> *cAbAg*, where *cAb* is the loaded antibody concentration, *cAg* is the

delivered analyte concentration, and *cAbAg* is the coupled analyte-antibody pair. The reaction association and dissociation rates are 10^5 $L \cdot mol^{-1}s^{-1}$ and 10^{-5} s^{-1} respectively. The analyte concentration was set to 300ng/mL and antibody concentration was 9.01 mg/mL. For simplicity, the loaded antibody and bound pair concentrations were normalized to the inlet analyte concentration. Particle image velocimetry (PIV) studies on the platform have been conducted to confirm the flow profiles from CFD and the flow patterns presented here compare well with those obtained from the experimental PIV (data not shown).

3. Results and Discussions

3.1 The fabrication of silicon taste-chip

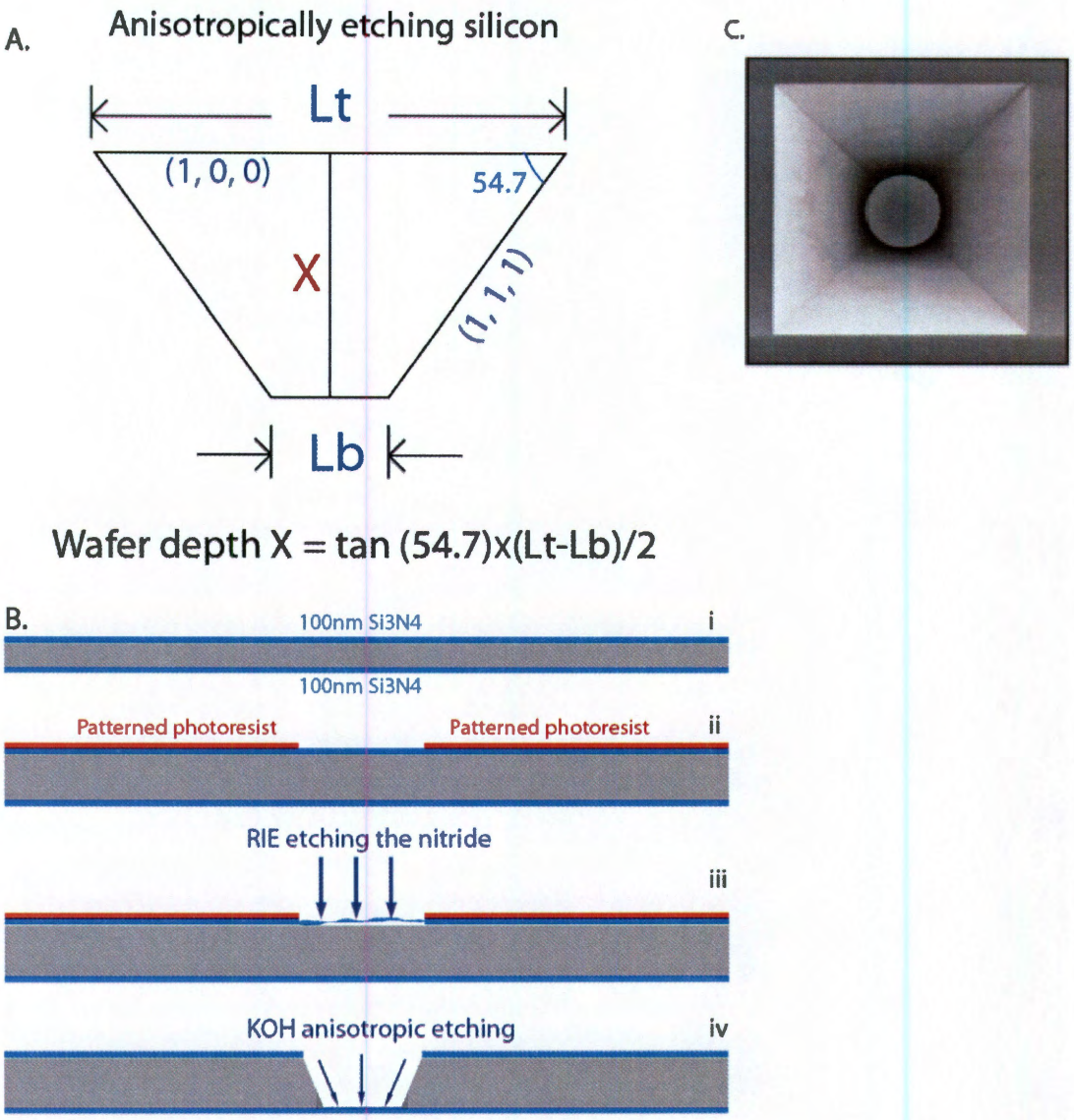

Figure 3 (A) Schematic of silicon crystal structure. (B) The wet etching process on the (1 0 0) silicon surface. (C) The SEM image of an etched microwell with a glass bead sitting inside.

A typical silicon taste chip as in Figure 3, is made through bulk micromachining of silicon using anisotropic etching. Inverted square- based pyramid wells are chemically etched in a square arrayed pattern on silicon wafers (230–380 μm thick). This design serves as a chamber to contain the beaded sensing element while allowing both bottom-illuminated light to be transmitted through the bead and fluid to flow perpendicular through the wafer. Furthermore, patterns of these wells have been etched to create 3 × 3, 3 × 4, 4 × 5, 5 × 7, or 10 × 10 arrays.

Although not fully understood (parameters such as atomic lattice packing density and attached H_2O molecules play an important role), anisotropic etching of silicon is characterized with the very highly preferential etching of silicon along the (111) surface, allowing the fabrication of microstructures with a great level of control. The complete sequence is shown in Figure 2. Briefly, here is the succession of steps required for the fabrication 280-μm double-sided polished p-type 4 inches single crystal silicon (1 0 0) wafer was deposited with Si_3N_4 using low-pressure chemical vapor deposition (LPCVD) techniques. A layer of ~1000 Å is created by reacting ammonia (NH_3) and dichlorosilane ($SiCl_2H_2$) gas with a flow rate of 3.5:1, i.e., 70:20 cm^3/min, at 830 °C and 200 mtorr. The wafer is then moved to a photolithography clean rom environment. The mask layer is removed from one side of the silicon substrate by protecting the other side with photoresist and plasma-etching (CF_4 and O_2 at 100W) the Si_3N_4 layer. This is achieved by reactive ion etching (RIE) with a flow rate of 20:1 CF_4:O_2 (80:4 cm^3/min). An etching rate of

~1000 Å/min is observed with 100 W of radio-frequency power and 50 mtorr of pressure.

The wafer is dipped into a 40% KOH solution at 79 °C for 9 hours in order to etch the substrate. This creates the square-based pyramidal wells with an angle of 54.7° with respect to the surface of the silicon. Once the KOH etch is completed, the nitride masking layer is completely removed with plasma etching.

To get rid of the reflectance from the substrate, the wafer is soaked in 30% H_2O_2 solution for 15-20 min to form a thin SiO_2 layer on the surface of the silicon. This improves surface-wetting characteristics.

3.2 PDMS-Thiolene hybrid chip design and fabrication

The hybrid chip is composed of three layers (Figure 4). The top and bottom PDMS layers contain the injection and drain channels respectively. The channels (300 μm wide, 50 μm high) were molded with SU8-2015 and cast into PDMS. The middle layer was an optical epoxy film with square pyramidal cavities, where the beads were physically constrained. Optically transparent epoxy provides light transmission in a wide spectrum range. The low background noise becomes an important feature when dealing with complex biological matrices, such as blood and saliva.

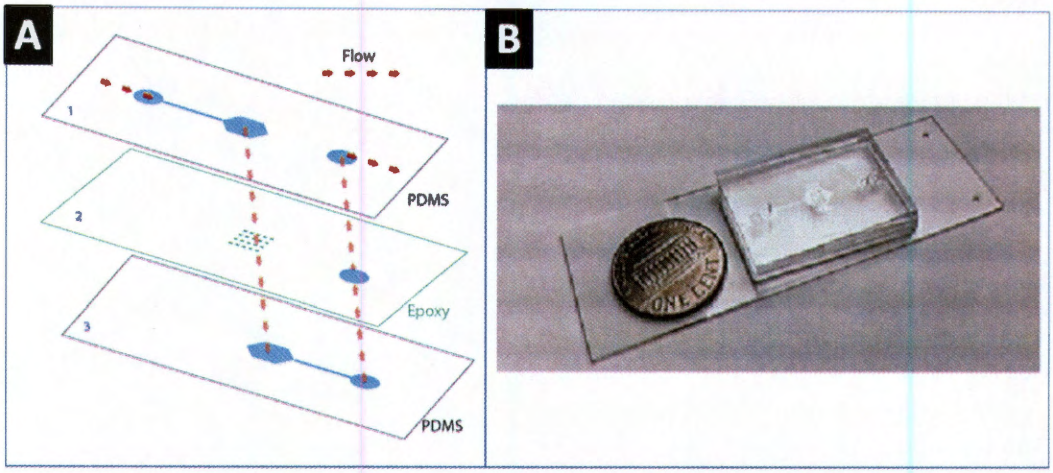

Figure 4 (A) The layout of the bio-nano-chip design. (B) The PDMS-thiolene hybrid chip with a U.S. penny.

The following steps were taken to achieve the pyramidal holes in the thiolene-based epoxy, as in Figure 4(A). First, a 400μm-thick silicon wafer with the <100> crystal surface orientation was prepared through anisotropic etching, as reported previously (Christodoulides et al. 2007), to create square pyramids with dimension at the top of 670μm and bottom 80μm as in Figure 4(B). Second, PDMS is casted on the silicon master to get a replica with positive features of the square pyramids. Then, NOA81 optical liquid adhesive is dispensed on the PDMS surface that has positive features and spun at 3.3 g units for 30 sec. The NOA81 chosen in this study has relatively low viscosity (300 cps), and therefore it easily spreads to a thin film without any air bubbles by spinning. However, because the PDMS surface is naturally hydrophobic, the liquid adhesive tends to aggregate together and form droplets on its surface, rather than spread out evenly, before spinning we need first utilize oxygen plasma (PE-50, Plasma Etch) and 2-hydroxyethyl methacrylate

(HEMA) polymer grafting to render its surface permanently hydrophilic (Bodas and Khan-Malek 2006). Finally, the composite was exposed in UV light for 1 min (Polylux 500, Norland Products). After the UV treatment, the liquid epoxy turns to a hard resilient solid film that could be peeled off easily from the PDMS. As displayed in Figure4(C), the replication from silicon to epoxy was accurate in terms of the square pyramidal shape. The bottom of the pyramid was found to be enlarged by about 50 μm due to the need to keep the level of epoxy liquid lower than the peak of positive PDMS replica after spinning, in order to produce through holes. A single piece of PDMS replica could be reused to produce a number of epoxy copies.

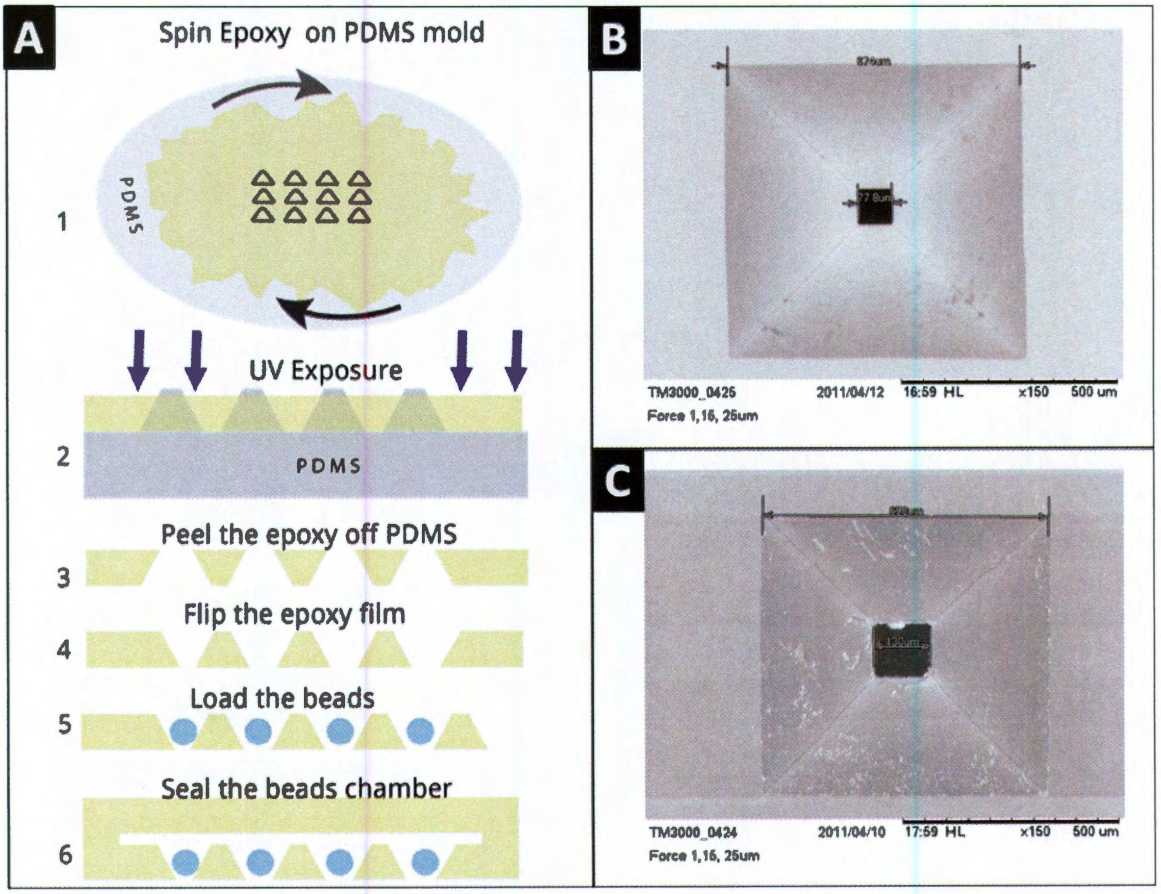

Figure 5 (A) Fabrication process of bead holders with the optical epoxy. (1) Spreading the epoxy over the PDMS replica of anisotropically etched silicon wafer. (2) Curing epoxy under the UV treatment. (3) Taking the PDMS and epoxy apart. (4) Attaching the bottom of epoxy film to the PDMS layer containing the drain. (5) Arranging the beads into the wells by tweezers. (6) Sealing the bead array by the PDMS layer containing the sample delivery channel. (B) SEM image on a silicon pyramidal cavity. The scale bar is 500μm. (C) SEM image on the epoxy cavity replicated from the silicon mold. The scale bar is 500μm.

The thiolene based epoxy could be bonded to PDMS by plasma cleaning (Hung et al. 2008). However, the general plasma cleaning protocol of bonding(Sunkara et al. 2010; Tang and Lee 2010). It takes advantage of the irreversible covalent bonding between plasma treated PDMS and the 3-aminopropyltriethoxysilane (APTES) modified thermoplastic surface (Figure 6). Here, we applied a similar technique to the surface of epoxy. First, the surface of epoxy was cleaned by oxygen plasma and then soaked in 1% v/v APTES solution for 30 min and dried with nitrogen. Second, agarose beads conjugated with anti-CRP antibodies were loaded into the wells manually with tweezers. Finally, the epoxy surface was brought into contact with the plasma cleaned PDMS surface, resulting into irreversible covalent bonding at RT. PDMS may not be suitable when agarose beads located on its surface. To ensure the polymeric bead structure stability, the

protein-derivatized agarose beads need be kept wetted all the time. On one hand, if the beads were loaded before plasma cleaning, the vacuum environment would dry out the agarose beads and denature the antibodies. On the other hand, if beads were loaded after plasma cleaning, the time required to load beads onto the array, would make it hard to exploit the best timeframe for bonding to take effect, which is immediately after treatment of the epoxy surface. Recently, a new way of bonding PDMS to thermoplastics at RT has been reported (Sunkara et al. 2010; Tang and Lee 2010). It takes advantage of the irreversible covalent bonding between plasma treated PDMS and the 3-aminopropyltriethoxysilane (APTES) modified thermoplastic surface (Figure 6). Here, we applied a similar technique to the surface of epoxy. First, the surface of epoxy was cleaned by oxygen plasma and then soaked in 1% v/v APTES solution for 30 min and dried with nitrogen. Second, agarose beads conjugated with anti-CRP antibodies were loaded into the wells manually with tweezers. Finally, the epoxy surface was brought into contact with the plasma cleaned PDMS surface, resulting into irreversible covalent bonding at RT.

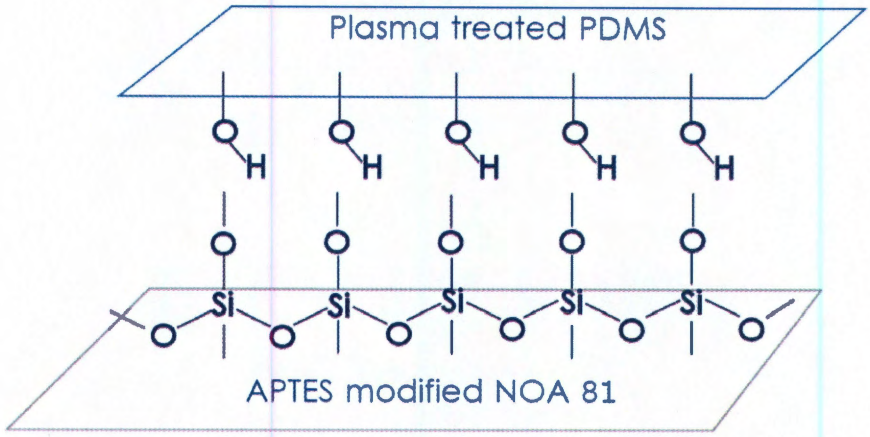

Figure 6 Room temperature bonding between APTES modified epoxy and plasma treated PDMS

3.3 CRP immunoassay within BNC

The inverted pyramidal microwells within the BNC serve both as reaction and analysis chambers. In a typical assay procedure, sample and reagent solutions are delivered around and through the beads, and then exit the chip through a drain, as illustrated in Figure 1. The microchip architecture largely enhances the mixing and reactions between analytes/ detection antibodies and therefore sensitivities (Goodey et al. 2001; Li et al. 2005).

The assay procedure was optimized by varying the sample and reagent volumes as well as the assay incubation times. Optimal conditions identified for this setup included incubation of CRP antigen for 30min at flow rate of 80 µL/min, followed by 30 min incubation with AlexaFluor®488-conjugated detection antibody

also delivered at 80 μL/min for 30 min. Following the incubation of detection antibody, the chamber and beads contained within were rinsed with PBS at 120 μL/min for 3 min to remove non-specific binding of reagents.

The observed small intra-assay bead to bead variations arise from three main sources. First, according to the simulation data of computational fluid dynamics, as shown in Figure1(C) and (D), there is a minor pressure gradient across the bead array, with pressures dropping from the column closest to the inlet to the column closest to the outlet. Higher pressure results in more penetrations of both the antigen and detecting antibody into the agarose bead matrix, and hence stronger signals. Second, within the same column, signals could vary because of the slightly different drain sizes below beads, in other words, the bottom hole size of the reaction chamber. Drain size is important to the signal of bead since it also affects the pressure applied on the bead by creating complex local fluidic fields. In other words, both the location of bead in the array and the pressure on the bead could play important roles on the detected fluorescence intensity. In our experiments, and especially for multiplex experiments we always keep the arrangement of beads consistent with respect to analyte groups, and observe great reproducibility. Last, while tightly sieved, the agarose bead size distribution still displays a 5% CV (Wong 2007), contributing to signal variations in our experiments. Because smaller beads sit lower in the pyramidal wells than the larger beads, they receive higher pressures and therefore show stronger signals.

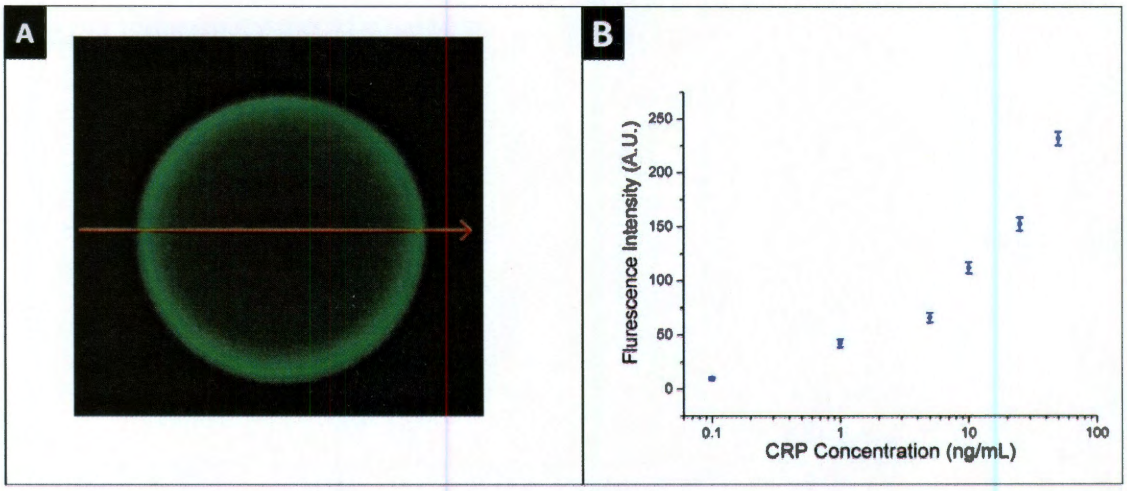

Figure 7 (A) Confocal fluorescence image of a bead after 25ng/mL CRP assays. (C) Dose response curve of CRP based on epi-fluorescence data.

3.4 Signals in agarose beads

The signal distribution was investigated by taking confocal images on a CRP bead at the end of the assay (Figure 7(A)). The PDMS chip was mounted on a glass slide and inverted on the stage for imaging from the objective from below. Medial slices of the beads in the x-y plane, with a 1μm thickness, at a distance of 140 μm from the top of the bead, were recorded as 8-bit in the green pseudo-color image of 510×510 pixels. The confocal data showed that signal mainly formed on the peripherals of beads and penetrated about 30% to the core of the beads (Figure 8). As compared to the solid phase polystyrene beads, where antigen-antibody interactions are confined on their 2D microsphere surfaces, the porous agarose

beads are capable to capture analytes in 3D shells with a thickness of about 100 μm, as we have previously demonstrated (Jokerst et al. 2011).

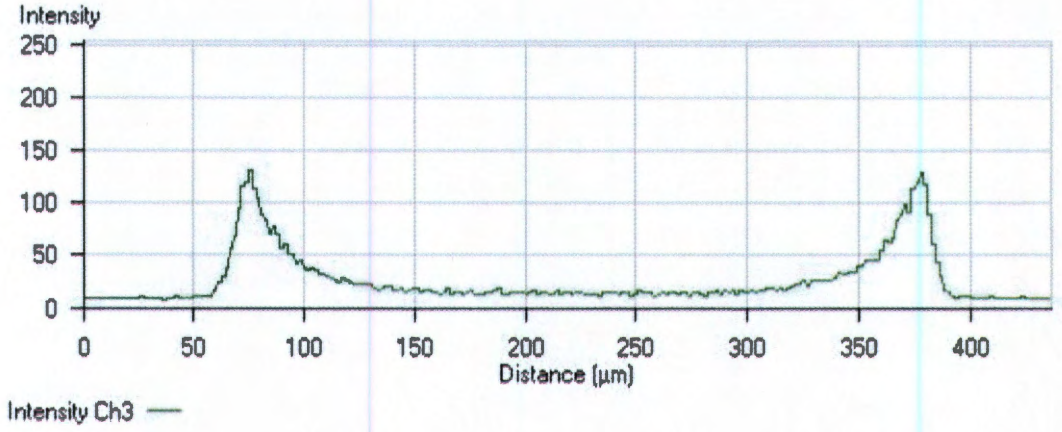

Figure 8 Fluorescence intensity profile recorded across the red arrow drawn in Figure 3(A).

3.5 Dose response curve

To gain a thorough understanding of the behavior of the platform when used in the multiplex, a necessary step is to investigate the behavior of array composed of identical beads, as to eliminate any possible influence of the differences between beads conjugated to different biological entities, with potentially different concentrations of capture antibody depending on the analytes, and possible interferences due to cross talk between the immunoassays. In Figure 3(B) is displayed a dose response curve of CRP, where each data point obtained by averaging nine beads for that concentration with error bars shown at ±1×SD. The redundancy of beads in the bead array helps acquire higher statistical significance, a

necessary requirement in the first investigative stages of any platform created through a new fabrication process. The limit of detection (LOD) was calculated at 1ng/mL, as the mean of the 0 antigen control run ±3×SD. While the physiological range for CRP measurements in blood extends to higher concentrations than the standards used in the dose response curve (Liu et al. 2010), we are targeting the detection of biomarkers in both blood and saliva (Floriano et al. 2009) in our clinical studies. As such, further dilutions by several orders of magnitude are often required for the more viscous and mucinous oral fluid, making it more strategic in assay development steps to target a wide range of lower concentrations. If necessary, a larger dynamic range is achieved easily by lowering or increasing the concentrations of detection antibody, as well as the exposure time for the CCD camera.

4. Conclusions

In summary, we have demonstrated the suitability of a cost-effective microfabrication methodology based on PDMS and thiolene-based optical epoxy to produce a new disposable bio-nano-chip design for lab-on-a-chip immunoassays. In this example demonstrated with a CRP immunoassay, analytes penetrated 100 μm into the core of 280 μm porous agarose beads and resulted in high sensitivity. Moreover, the fabrication process of the bio-nano-chip is repeatable and amenable to scale-up, thereby affording applications targeting resource-scarce settings. In

addition, the PDMS, a standard material in microfluidics, allows for a wide range of integration with new features and advances, which are constantly emerging from the microfluidic.

Reference

Ali, M.F., Kirby, R., Goodey, A.P., Rodriguez, M.D., Ellington, A.D., Neikirk, D.P., McDevitt, J.T., 2003. DNA Hybridization and Discrimination of Single-Nucleotide Mismatches Using Chip-Based Microbead Arrays. Analytical Chemistry 75(18), 4732-4739.

Bange, A., Halsall, H.B., Heineman, W.R., 2005. Microfluidic immunosensor systems. Biosensors and Bioelectronics 20(12), 2488-2503.

Bodas, D., Khan-Malek, C., 2006. Formation of more stable hydrophilic surfaces of PDMS by plasma and chemical treatments. Microelectronic Engineering 83(4-9), 1277-1279.

Christodoulides, N., Dharshan, P., Wong, J., Floriano, P.N., Neikirk, D., McDevitt, J.T., 2007. A microchip-based assay for interleukin-6. Methods in molecular biology 385, 131-144.

Christodoulides, N., Floriano, P.N., Acosta, S.A., Ballard, K.L.M., Weigum, S.E., Mohanty, S., Dharshan, P., Romanovicz, D., McDevitt, J.T., 2005a. Toward the Development of a Lab-on-a-Chip Dual-Function Leukocyte and C-Reactive Protein Analysis Method for the Assessment of Inflammation and Cardiac Risk. Clinical chemistry 51(12), 2391-2395.

Christodoulides, N., Mohanty, S., Miller, C.S., Langub, M.C., Floriano, P.N., Dharshan, P., Ali, M.F., Bernard, B., Romanovicz, D., Anslyn, E., Fox, P.C., McDevitt, J.T., 2005b. Application of microchip assay system for the measurement of C-reactive protein in human saliva. Lab on a Chip 5(3), 261-269.

Christodoulides, N., Tran, M., Floriano, P.N., Rodriguez, M., Goodey, A., Ali, M., Neikirk, D., McDevitt, J.T., 2002. A microchip-based multianalyte assay system for the assessment of cardiac risk. Analytical Chemistry 74(13), 3030-3036.

Floriano, P.N., Christodoulides, N., Miller, C.S., Ebersole, J.L., Spertus, J., Rose, B.G., Kinane, D.F., Novak, M.J., Steinhubl, S., Acosta, S., Mohanty, S., Dharshan, P., Yeh, C.-k., Redding, S., Furmaga, W., McDevitt, J.T., 2009. Use of Saliva-Based Nano-Biochip Tests for Acute Myocardial Infarction at the Point of Care: A Feasibility Study. Clinical chemistry 55(8), 1530-1538.

Fu, E., Lutz, B., Kauffman, P., Yager, P., 2010. Controlled reagent transport in disposable 2D paper networks. Lab on a Chip 10(7), 918-920.

Golden, J.P., Kim, J.S., Erickson, J.S., Hilliard, L.R., Howell, P.B., Anderson, G.P., Nasir, M., Ligler, F.S., 2009. Multi-wavelength microflow cytometer using groove-generated sheath flow. Lab on a Chip 9(13), 1942-1950.

Goodey, A., Lavigne, J.J., Savoy, S.M., Rodriguez, M.D., Curey, T., Tsao, A., Simmons, G., Wright, J., Yoo, S.-J., Sohn, Y., Anslyn, E.V., Shear, J.B., Neikirk, D.P., McDevitt, J.T., 2001. Development of Multianalyte Sensor Arrays Composed of Chemically Derivatized Polymeric Microspheres Localized in Micromachined Cavities. Journal of the American Chemical Society 123(11), 2559-2570.

Hung, L.-H., Lin, R., Lee, A.P., 2008. Rapid microfabrication of solvent-resistant biocompatible microfluidic devices. Lab on a Chip 8(6), 983-987.

Jokerst, J.V., Chou, J., Camp, J.P., Wong, J., Lennart, A., Pollard, A.A., Floriano, P.N., Christodoulides, N., Simmons, G.W., Zhou, Y., Ali, M.F., McDevitt, J.T., 2011.

Location of Biomarkers and Reagents within Agarose Beads of a Programmable Bio-nano-chip. Small 7(5), 613-624.

Jokerst, J.V., Floriano, P.N., Christodoulides, N., Simmons, G.W., McDevitt, J.T., 2008. Integration of semiconductor quantum dots into nano-bio-chip systems for enumeration of CD4+ T cell counts at the point-of-need. Lab on a Chip 8(12), 2079-2090.

Jokerst, J.V., Jacobson, J.W., Bhagwandin, B.D., Floriano, P.N., Christodoulides, N., McDevitt, J.T., 2010. Programmable Nano-Bio-Chip Sensors: Analytical Meets Clinical. Analytical Chemistry 82(5), 1571-1579.

Jokerst, J.V., Raamanathan, A., Christodoulides, N., Floriano, P.N., Pollard, A.A., Simmons, G.W., Wong, J., Gage, C., Furmaga, W.B., Redding, S.W., McDevitt, J.T., 2009. Nano-bio-chips for high performance multiplexed protein detection: Determinations of cancer biomarkers in serum and saliva using quantum dot bioconjugate labels. Biosensors & Bioelectronics 24(12), 3622-3629.

Kirby, R., Cho, E.J., Gehrke, B., Bayer, T., Park, Y.S., Neikirk, D.P., McDevitt, J.T., Ellington, A.D., 2004. Aptamer-Based Sensor Arrays for the Detection and Quantitation of Proteins. Analytical Chemistry 76(14), 4066-4075.

Lee, W.G., Kim, Y.-G., Chung, B.G., Demirci, U., Khademhosseini, A., 2010. Nano/Microfluidics for diagnosis of infectious diseases in developing countries. Advanced Drug Delivery Reviews 62(4-5), 449-457.

Li, S.F., Floriano, P.N., Christodoulides, N., Fozdar, D.Y., Shao, D.B., Ali, M.F., Dharshan, P., Mohanty, S., Neikirk, D., McDevitt, J.T., Chen, S.C., 2005. Disposable

polydimethylsiloxane/silicon hybrid chips for protein detection. Biosensors & Bioelectronics 21(4), 574-580.

Lim, C.T., Zhang, Y., 2007. Bead-based microfluidic immunoassays: The next generation. Biosensors and Bioelectronics 22(7), 1197-1204.

Liu, A., Bui, T., Van Nguyen, H., Ong, B., Shen, Q., Kamalasena, D., 2010. Serum C-reactive protein as a biomarker for early detection of bacterial infection in the older patient. Age and Ageing 39(5), 559-565.

Meagher, R.J., Hatch, A.V., Renzi, R.F., Singh, A.K., 2008. An integrated microfluidic platform for sensitive and rapid detection of biological toxins. Lab on a Chip 8(12), 2046-2053.

Moon, S., Keles, H.O., Ozcan, A., Khademhosseini, A., Hæggstrom, E., Kuritzkes, D., Demirci, U., 2009. Integrating microfluidics and lensless imaging for point-of-care testing. Biosensors and Bioelectronics 24(11), 3208-3214.

Nolan, J.P., Sklar, L.A., 2002. Suspension array technology: evolution of the flat-array paradigm. Trends in biotechnology 20(1), 9-12.

Pregibon, D.C., Toner, M., Doyle, P.S., 2007. Multifunctional Encoded Particles for High-Throughput Biomolecule Analysis. Science 315(5817), 1393-1396.

Shin, K.-S., Lee, S.W., Han, K.-C., Kim, S.K., Yang, E.K., Park, J.H., Ju, B.-K., Kang, J.Y., Kim, T.S., 2007. Amplification of fluorescence with packed beads to enhance the sensitivity of miniaturized detection in microfluidic chip. Biosensors and Bioelectronics 22(9-10), 2261-2267.

Sia, S.K., Kricka, L.J., 2008. Microfluidics and point-of-care testing. Lab on a Chip 8(12), 1982-1983.

Sia, S.K., Linder, V., Parviz, B.A., Siegel, A., Whitesides, G.M., 2004. An Integrated Approach to a Portable and Low-Cost Immunoassay for Resource-Poor Settings. Angewandte Chemie International Edition 43(4), 498-502.

Sohn, Y.-S., Goodey, A., Anslyn, E.V., McDevitt, J.T., Shear, J.B., Neikirk, D.P., 2005. A microbead array chemical sensor using capillary-based sample introduction: toward the development of an "electronic tongue". Biosensors and Bioelectronics 21(2), 303-312.

Sunkara, V., Park, D.-K., Hwang, H., Chantiwas, R., Soper, S.A., Cho, Y.-K., 2010. Simple room temperature bonding of thermoplastics and poly(dimethylsiloxane). Lab on a Chip 11(5), 962-965.

Tang, L., Lee, N.Y., 2010. A facile route for irreversible bonding of plastic-PDMS hybrid microdevices at room temperature. Lab on a Chip 10(10), 1274-1280.

Thompson, J.A., Bau, H.H., 2010. Microfluidic, bead-based assay: Theory and experiments. Journal of Chromatography B 878(2), 228-236.

Thompson, J.A., Du, X.G., Grogan, J.M., Schrlau, M.G., Bau, H.H., 2010. Polymeric microbead arrays for microfluidic applications. Journal of Micromechanics and Microengineering 20(11), 115017-115025.

Walt, D.R., 2005. Miniature Analytical Methods for Medical Diagnostics. Science 308(5719), 217-219.

Wong, J., 2007. Bead based microreactors for sensing applications. Ph.D. dissertation, The University of Texas at Austin.

Yager, P., Edwards, T., Fu, E., Helton, K., Nelson, K., Tam, M.R., Weigl, B.H., 2006. Microfluidic diagnostic technologies for global public health. Nature 442(7101), 412-418.